British Journal of Pharmacology (2008) 155, 1127–1138

0007–1188/08 $32.00
www.brjpharmacol.org

RESEARCH PAPER

# Impact of efflux transporters and of seizures on the pharmacokinetics of oxcarbazepine metabolite in the rat brain

R Clinckers[1,2], I Smolders[1], Y Michotte[1], G Ebinger[3], M Danhof[2], RA Voskuyl[2] and O Della Pasqua[2]

[1]*Department of Pharmaceutical Chemistry and Drug Analysis (labo FASC), Farmaceutisch Instituut—Gebouw G, Vrije Universiteit Brussel (VUB), Brussels, Belgium;* [2]*Division of Pharmacology, Leiden/Amsterdam Center for Drug Research (LACDR), Leiden University, Leiden, The Netherlands and* [3]*Department of Neurology, University Hospital UZ-Brussels, Brussels, Belgium*

**Background and purpose:** Accurate prediction of biophase pharmacokinetics (PK) is essential to optimize pharmacotherapy in epilepsy. Here, we characterized the PK of the active metabolite of oxcarbazepine, 10,11-dihydro-10-hydroxy-carbamazepine (MHD) in plasma and in the hippocampus. Simultaneously, the impact of acute seizures and efflux transport mechanisms on brain distribution was quantified.
**Experimental approach:** Rats received subtherapeutic and anticonvulsant doses of MHD in non-epileptic conditions and during focal pilocarpine-induced limbic seizures. To evaluate the effect of efflux transport blockade, a separate group received subtherapeutic doses combined with intrahippocampal perfusion of verapamil. Free plasma and extracellular hippocampal MHD concentrations were determined using microdialysis and liquid chromatography techniques. An integrated PK model describing simultaneously the PK of MHD in plasma and brain was developed using nonlinear mixed effects modelling. A bootstrap procedure and a visual predictive check were performed to assess model performance.
**Key results:** A compartmental model with combined zero- and first-order absorption, including lag time and biophase distribution best described the PK of MHD. A distributional process appeared to underlie the increased brain MHD concentrations observed following seizure activity and efflux transport inhibition, as reflected by changes in the volume of distribution of the biophase compartment. In contrast, no changes were observed in plasma PK.
**Conclusions and implications:** Simultaneous PK modelling of plasma and brain concentrations has not been used previously in the evaluation of antiepileptic drugs (AEDs). Characterisation of biophase PK is critical to assess the impact of efflux transport mechanisms and acute seizures on brain disposition and, consequently, on AED effects.
*British Journal of Pharmacology* (2008) **155,** 1127–1138; doi:10.1038/bjp.2008.366; published online 6 October 2008

**Keywords:** population pharmacokinetic modelling; NONMEM; 10,11-dihydro-10-hydroxy-carbamazepine; epilepsy; efflux transport; biophase kinetics; microdialysis

**Abbreviations:** AEDs, antiepileptic drugs; BBB, blood–brain barrier; EC, extracellular; ECF, extracellular fluid; mCBZ, 2-methyl-5*H*-dibenz(*b*,*f*)azepine-5-carboxamide; MHD, 10,11-dihydro-10-hydroxy-carbamazepine; PD, pharmacodynamic(s); PK, pharmacokinetic(s); VPC, visual posterior predictive check

## Introduction

Despite considerable progress in the pharmacotherapy of epilepsy during the last decades, the problem of intractable seizures has not changed on the introduction of new antiepileptic drugs (AEDs) (Löscher, 2002). Just as epilepsy itself is a heterogeneous condition with multiple aetiologies, the pathogenesis of refractoriness is considered to be multifactorial and variable. Evidence from ongoing research suggests that epilepsy-related pharmacodynamic (PD) and pharmacokinetic (PK) changes may lie at the basis of the development of pharmacoresistance. A crucial determinant in the PK hypothesis for pharmacoresistance is represented by the blood–brain barrier (BBB), which is considered to govern drug access to the biophase and hence alter bioavailability in the brain.

Following BBB penetration, a compound may distribute into the extracellular (EC), intracellular and CSF fluid compartments depending on its physicochemical properties. As the brain may not be considered *a priori* a homogeneous

Correspondence: Dr O Della Pasqua, Division of Pharmacology, Leiden/Amsterdam Center for Drug Research (LACDR), Gorlaeus Laboratories Einsteinweg, Leiden University, 55 PO Box 9502, Leiden 2300 RA, Netherlands.
E-mail: odp72514@gsk.com
Received 17 March 2008; revised 26 June 2008; accepted 7 August 2008; published online 6 October 2008

compartment, drug distribution may vary among brain areas (de Lange and Danhof, 2002). Multiple factors govern drug distribution into and within brain compartments, some of which can be affected during pathological conditions. Pathological conditions of the CNS, such as the epilepsies, are known to compromise the integrity and selective permeability of the BBB in epileptogenic areas, causing regional concentration differences within the brain (Oby and Janigro, 2006). On the other hand, several classes of efflux transporters are present on brain capillary endothelial cells and strengthen the physical barrier function of the BBB (Kwan and Brodie, 2005; Löscher and Potschka, 2005). Overexpression of active efflux mechanisms has been described in epileptic brain areas and is suggested to have a substantial function in therapeutic failure to antiepileptic pharmacological treatment (Clinckers *et al*., 2005; Löscher and Potschka, 2005; van Vliet *et al*., 2007). Active efflux transporters are also expressed at the cellular membranes of parenchymal cells such as microglia and astrocytes and are considered to act in tandem with transport systems at the BBB in hindering efficient drug delivery to the brain (Scism *et al*., 2000; Lee *et al*., 2001).

To date, an integrated, quantitative evaluation is lacking of how seizures and active efflux transport mechanisms modify the biophase PK of AEDs and consequently, their effects. To study the influence of active efflux mechanisms on brain drug disposition *in vivo*, intracerebral microdialysis is a valuable technique. It allows investigation of BBB transport characteristics and brain distribution of CNS drugs as a function of time, as reflected by free drug concentrations in the EC fluid (ECF). For many CNS active drugs, it is accepted that EC brain concentrations are most closely related to the biophase concentrations. The microdialysis technique offers, therefore, an opportunity for the use of mechanism-based PK/PD modelling for prediction and optimization of therapeutic regimens of AEDs (Danhof *et al*., 2008). Furthermore, the technique also allows *in situ* application of compounds to study their local effects.

The present population PK modelling study was aimed at characterising, in an integrated manner, the PK of 10,11-dihydro-10-hydroxy-carbamazepine (MHD), the active metabolite of oxcarbazepine, in rat plasma and brain in control conditions and during acute limbic seizures. The impact of efflux inhibition on MHD biophase equilibration was assessed by co-administration *in situ* of the efflux transport-blocking agent verapamil. Verapamil is an extensively used non-selective multidrug resistance modulator, which has often been used as a standard P-glycoprotein-blocking agent in various tissues including the brain (Bebawy *et al*., 2001). Although systemic verapamil administration may seem clinically most relevant, this approach does not allow drawing clear-cut conclusions about BBB efflux mechanisms in the brain. In fact, brain disposition may be indirectly affected by changes in plasma PK following systemic administration of an efflux transport inhibitor. In contrast to previous investigations, in which the time course of drug concentration in plasma and brain were always modelled separately, here we analyse the data from all treatment groups simultaneously. A key advantage of a combined modelling approach is the possibility to discriminate between two possibilities; that the differences in brain concentrations are strictly related to altered BBB transport or that they are due to variations in systemic drug disposition. The proposed population modelling approach enables accurate prediction of plasma and brain MHD concentrations and quantifies the impact of efflux transport inhibition and acute seizures on MHD brain disposition.

## Methods

*Animals*

All animal experiments described in this article were carried out according to the European Guidelines on Animal Experimentation and were approved by the Ethical Committee of the Free University of Brussels. Male Wistar albino rats weighing between 260 and 320 g (Iffa Credo, Brussels, Belgium) were housed in groups for at least 7 days following arrival in the animal facilities. Standard environmental conditions were ensured (temperature 21 °C, humidity 60%, 12/12 h dark–light cycle, lights on at 0700 hours). During the actual experimental procedures, rats were placed in experimental cages and allowed to move freely. All animals had access to tap water and standard laboratory chow *ad libitum*.

*Surgical procedures*

Rats were anaesthetized with a mixture of ketamine HCl and diazepam (58 and 4.5 mg kg$^{-1}$, respectively). A CMA/12 guide cannula with a replaceable inner guide (CMA Microdialysis, Solna, Sweden) was implanted stereotaxically in the hippocampus, 3 mm above the final probe membrane position (CA1–CA3 region). The hippocampus was selected as target region because it is the region in the brain that is most susceptible to seizures and is often the site of epileptic foci in limbic epilepsies. Moreover, efflux transporter overexpression after status epilepticus induction by perforant path stimulation was recently shown to be region specific and restricted to the ventral hippocampus and para-hippocampal cortex (van Vliet *et al*., 2007). The cannula was fixed to the skull with dental acrylic cement. The coordinates were 4.6 mm lateral and 5.6 mm posterior to bregma and 4.6 mm ventral starting from the dura (Paxinos and Watson, 1986). Serial blood samples were collected through an indwelling cannula in the right femoral artery. Cannulae (i.d. = 0.58 mm; o.d. = 0.96 mm) were made from 20 cm pyrogen-free polyethylene tubing (Portex Limited, Hythe, Kent, UK), subcutaneously tunnelled to the back of the neck of the rats and exteriorized. The arterial cannula was filled with saline containing 50 IU mL$^{-1}$ heparin to prevent clotting. Postoperative analgesia was assured by a single injection of ketoprofen (4 mg kg$^{-1}$ i.p.). Immediately after surgery, a 3 mm CMA12 microdialysis probe (CMA Microdialysis) was inserted. The probes consist of a polycarbonate-polyether copolymeric membrane with a molecular cut-off of 20 kDa. The probe was continuously perfused (flow rate 2 μL min$^{-1}$) with modified Ringer's solution, containing 147 mM NaCl, 2.3 mM $CaCl_2$ and 4 mM KCl. The rats used for the assessment of the impact of efflux transport mechanisms on brain

disposition had a second microdialysis probe implanted into the contralateral hippocampus. The coordinates were −4.6 mm lateral and 5.6 mm posterior to bregma and 4.6 mm ventral starting from the dura (Paxinos and Watson, 1986).

*Study design*

Rats were randomly allocated to different treatment groups (see Table 1). To study the impact of acute seizures, the chemoconvulsant muscarinic agonist pilocarpine was perfused intrahippocampally through a microdialysis probe (10 mM for 40 min at 2 μL min$^{-1}$). The influence of efflux transport inhibition on MHD distribution to the brain was investigated in a separate experiment, in which animals received continuous unilateral intrahippocampal perfusion of verapamil (5 mm at 2 μL min$^{-1}$). In the latter experimental group, the contralateral hippocampus served as a control. Blood samples and brain microdialysates were collected prior and at various time points after MHD administration. Microdialysate samples were also used to determine EC brain monoamine neurotransmitter levels. The PD data were collected to characterize the PK–PD relationship of MHD on brain monoamines, which will be discussed in a separate publication.

*Experimental procedures*

The experimental protocol was started at a minimum of 16 h after surgery to allow the animals to recover sufficiently. Although tissue injury is unavoidable in the vicinity of implanted microdialysis probes, most of the tissue properties remain intact and BBB integrity is restored after 30 min (Benveniste and Hüttemeier, 1990; Clapp-Lilly *et al.*, 1999). All experiments were started between 0900 and 0930 hours. The internal reference/standard technique (Larsson, 1991; Scheller and Kolb, 1991) was used as *in vivo* calibration method for the determination of the microdialysis probe recovery of each dialysate sample. The method allows immediate detection of and correction for differences in probe recovery due to changes in tissue or probe characteristics. 2-Methyl-5*H*-dibenz(*b*,*f*)azepine-5-carboxamide (mCBZ) was used as the internal standard because of its structural similarity to MHD and because it does not interfere with the pathophysiology of epilepsy (unpublished observation). The internal standard (1 μg mL$^{-1}$) was added to the perfusion fluid 30 min before the start of the experiment to allow the establishment of dialysis equilibrium. At the same time, a blank arterial blood sample was collected. At the start of the experiment, rats received an i.p. bolus injection of MHD. A broad range of MHD doses (20–150 mg kg$^{-1}$) was used to enable accurate evaluation of PK properties (Table 1). MHD was suspended in a mixture of propylene glycol, ethanol and saline (6:2:2). After 30 min, convulsions were provoked by adding pilocarpine to the perfusion fluid for 40 min. During the experiment, the perfusion flow rate was kept constant at 2 μL min$^{-1}$ with a pulse-free pump (CMA 100 microdialysis pump; CMA Microdialysis). For determination of EC hippocampal MHD concentrations, microdialysis samples were collected every 20 min, except for the four samples immediately after MHD administration, which were collected at 10-min intervals. The sampling times were time averaged and corrected for dialysis lag time (4 min). At pre-defined time points, serial arterial blood samples (200 μL) were taken to determine MHD plasma concentrations. The total blood sample volume collected did not exceed 2.0 mL and was reconstituted with physiological saline solution. Blood samples were collected in 1.5 mL polypropylene tubes (Eppendorf, Hamburg, Germany) containing 40 μL EDTA (2.2 g%) and centrifuged at 385 *g* for 15 min at 37 °C for plasma collection. The sampling intervals correspond to the time-averaged and lag-time-corrected microdialysis sampling times. Plasma (100 μL) was subsequently ultrafiltrated (Vivaspin 0.5 mL concentrator, 5000 MW cutoff PES; Vivascience AG, Hannover, Germany) at 1800 *g* for 15 min to obtain free MHD concentrations. Ultrafiltration parameters were optimized yielding 96% recovery or more. Microdialysate and ultrafiltrate samples were kept frozen at −20 °C until assay.

The same protocol procedures were applied to evaluate the impact of efflux transport inhibition on hippocampal MHD distribution. MHD was administered as an i.p bolus at a dose of 20 mg kg$^{-1}$ ($n = 4$). Verapamil (5 mM; $K_i = 30$ μM) was included in the perfusion fluid of the left hippocampal probe for *in situ* efflux transport blockade. Verapamil perfusion was initiated together with the mCBZ perfusion. The right hippocampal probe served as a control (that is, no verapamil was added to the dialysate). An illustration of the probe position and experimental design is presented in Figure 1.

**Table 1** Treatment groups

| *MHD dose (mg kg$^{-1}$)* | *Intrahippocampal administration* | *N* |
|---|---|---|
| 20 | Vehicle | 2 + 4[a] |
| | 10 mM pilocarpine | 2[b] |
| | 5 mM verapamil | 4[a] |
| 40 | Vehicle | 2 |
| | 10 mM pilocarpine | 3[b] |
| 60 | Vehicle | 4 |
| | 10 mM pilocarpine | 2[b] |
| 80 | Vehicle | 2 |
| | 10 mM pilocarpine | 6 |
| 100 | Vehicle | 2 |
| | 10 mM pilocarpine | 4 |
| 150 | Vehicle | 2 |
| | 10 mM pilocarpine | 5 |

Abbreviations: MHD, 10,11-dihydro-10-hydroxy-carbamazepine; *N*, number of rats.
[a]Data obtained by dual probe technique performed in the same animal: ipsilateral, verapamil perfusion; contralateral, vehicle perfusion.
[b]Rats with acute seizures.

*Drug analysis*

MHD and mCBZ concentrations were analysed with an off-line microbore (100 mm × 1 mm i.d.) isocratic liquid chromatography assay coupled to a U-shaped high-sensitivity UV optical cell (cell volume 70 nL; optical path length 8 mm)

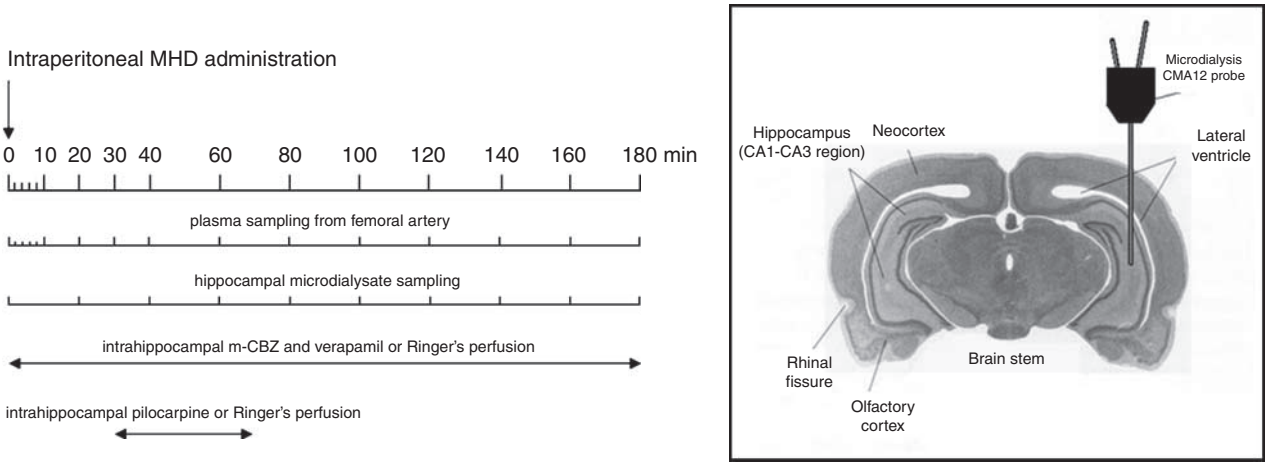


**Figure 1** Experimental set-up. Timescale showing plasma and dialysate collection time intervals (in minutes) and continuous perfusion periods for the different intrahippocampally applied compounds. Microdialysis probe position is schematically depicted in the hippocampal CA1–CA3 region.

(Van Belle *et al*., 1995). The liquid chromatography-UV system consisted of a Gilson 307 piston pump (Gilson SAS, Villiers le Bel, France). The inlet of the UniJet microbore column (C8, 5 μm; 150 mm × 1 mm; Unijet, Bioanalytical Systems, West Lafayette, IN, USA) equipped with a guard column was connected to a Gilson 231 XL sampling injector (Gilson SAS), and the outlet to a Kontron 433 capillary detector cell (LC Packings, Amsterdam, The Netherlands). The mobile phase consisted of filtered (0.2 μm filter) water and acetonitrile (73:27). The flow rate over the column was 60 μL min$^{-1}$. For both compounds, the limit of quantification was 5 ng mL$^{-1}$.

*Data analysis*

Nonlinear mixed-effects modelling as implemented in the NONMEM software package (version V, level 1.1) (Beal and Sheiner, 1999) was used to characterize the PK of MHD in rat plasma and hippocampal EC fluid simultaneously. A detailed background of population modelling is described elsewhere (Sheiner and Grasela, 1991). Final model parameters were estimated using the first-order conditional estimation method with $\eta$–$\varepsilon$ interaction (FOCE interaction). This approach allows the estimation of inter- and intra-subject variability in model parameters. All fitting procedures were performed on an IBM-compatible computer (Pentium IV, 1500 MHz) running under Windows XP. The Fortran compiler Compaq Visual Fortran version 6.1 was used for compilation. The R interface was used for data and bootstrap analysis. GraphPad Prism 4.0 (San Diego, CA, USA) was used for graphical display of the data.

*Simultaneous analysis of MHD PK in plasma and brain*

One-, two- and three-compartment models with linear and nonlinear elimination were tested. Model building and model selection were based on the likelihood ratio test, goodness-of-fit plots, parameter point estimates with their respective 95% confidence intervals and parameter correlations. For the likelihood ratio test, the significance level was set at $\alpha = 0.01$, which corresponds to a decrease of 6.6 points in the minimum value of the objective function after the inclusion of one parameter, under the assumption that the difference in minimum value of the objective function between two nested models is $\chi^2$-distributed (Wählby *et al*., 2001). Goodness-of-fits was evaluated by diagnostic plots and bootstrapping. Diagnostic plots included the assessment of conditional weighed residuals (Hooker *et al*., 2007).

The ADVAN6 subroutine in NONMEM was used for the purposes of this analysis. The PK model was parameterized in terms of rate constants and volumes of distribution (Figure 1). The stochastic part of the model assumed a log-normal distribution for the inter-subject variability in PK parameters:

$$P_i = \theta_i \exp(\eta_i) \quad (1)$$

with

$$\eta_i \sim N(0, \omega^2) \quad (2)$$

where $P_i$ is the individual estimate, $\theta$ is the population value (typical value) of parameter $P$ and $\eta_i$ is the normally distributed inter-individual random variable with mean zero and variance $\omega^2$. The coefficient of variation for fixed effects (that is, structural model parameters) is expressed as a percentage of the root mean square of the inter-individual variance term.

The influence of seizures and co-infusion of verapamil on the disposition of MHD was evaluated using stepwise covariate inclusion according to the following equation:

$$P_i = \theta_1 AB + \theta_2(1-A)B + \theta_3(1-A)(1-B) \quad (3)$$

in which $A$ and $B$ are flags for experimental conditions. Both $A$ and $B$ were set to 1 in control animals; to 0 and 1, respectively, in seizing animals; and 1 and 0, respectively, in verapamil-treated animals. The likelihood ratio test and diagnostic plots were used to assess the statistical significance of covariate inclusion.

Selection of the appropriate residual error model was based on the inspection of the goodness-of-fit plots. Residual variability for PK in plasma was characterized by a combination of a proportional and an additive error factor.

$$C_{\mathrm{obs},ij} = C_{\mathrm{pred},ij}(1 + \varepsilon_{1ij}) + \varepsilon_{2ij} \quad (4)$$

where $C_{\mathrm{obs},ij}$ is the *j*th observed plasma concentration in the *i*th individual and $C_{\mathrm{pred},ij}$ is the plasma concentration predicted by the model. $\varepsilon_{1ij}$ and $\varepsilon_{2ij}$ account for the deviation from the predicted concentration at any given time point. The value for $\varepsilon$ was assumed to be independently normally distributed with mean zero and variance $\sigma^2$.

Residual variability for MHD PK in brain was described according to a proportional error model.

$$C_{\mathrm{obs},ij} = C_{\mathrm{pred},ij} + \varepsilon_{ij}.\sqrt{1 + \mathrm{WT}^2 C_{\mathrm{pred},ij^2}} \quad (5)$$

where WT is a weighing factor. The residual error term accounts for unexplainable errors, which were assumed to be different from the residual variability in plasma PK.

The performance and precision of the final PK model were investigated by an internal validation method, which consisted of a non-parametric bootstrap analysis and visual posterior predictive check (VPC) (Iwi *et al*., 1999; Yano *et al*., 2001; Ette *et al*., 2003). This validation approach assesses whether parameter estimates are well estimated and accurately predicts the time course of MHD concentrations in plasma and hippocampal ECF. In the bootstrap analysis, a new randomly sampled replicate of the original data set is obtained (that is, a bootstrap sample) with replacement (Iwi *et al*., 1999). The final population PK model was re-fitted to each of the bootstrap replicates one at a time and this process was repeated 1500 times with different random draws. Bootstrap runs with unsuccessful minimization were excluded from further analysis. The stability of the model was evaluated by visual inspection of the distribution of the model parameter estimates from the new data sets and compared with that obtained from the fit of the original data set. The final PK parameter estimates were compared with the mean parameter estimates obtained from the bootstrap replicates. A VPC was also performed. It consisted of a simulation of the population PK profiles for the different treatment protocols using final model parameters and construction of a non-parametric 95% prediction interval around the median MHD concentration to quantify the (inter-subject and residual) variability in the model predictions.

*Chemicals*

Pilocarpine HCl, (*RS*)-verapamil HCl and mCBZ were purchased from Sigma-Aldrich (Bornem, Belgium). MHD was kindly donated by Novartis Pharma AG (Basel, Switzerland). All other chemicals were analytical reagent grade or higher and were supplied by Merck (Darmstadt, Germany). Aqueous solutions were made with purified water (Seralpur pro 90 CN; Belgolabo, Overijse, Belgium) and filtered through a 0.2 μm membrane filter.

## Results

In vivo *microdialysis probe recoveries*

The mean (± s.e.mean) relative recovery and relative loss for MHD were 7.81 ± 0.80% ($n = 6$) and 8.07 ± 0.93% ($n = 6$), respectively. The average relative loss for mCBZ was 40.54 ± 1.27% ($n = 8$). These experimentally derived recoveries were used to calculate the real EC hippocampal MHD concentration in each dialysate collection according to the internal reference technique (Larsson, 1991; Scheller and Kolb, 1991). Verapamil and pilocarpine co-perfusion did not affect the *in vivo* probe recovery for MHD or mCBZ (data not shown).

*Anticonvulsant effects*

Administration of 20, 40 and 60 mg kg$^{-1}$ MHD did not prevent the development of pilocarpine-induced limbic seizure activity in rats. From 80 mg kg$^{-1}$ onwards, limbic seizure activity could be completely blocked. On the basis of these observations, a subtherapeutic dosing range (20–60 mg kg$^{-1}$) and an anticonvulsant dosing range (80–150 mg kg$^{-1}$) were defined (Table 1).

*Population PK model selection*

Figure 2 depicts the time course of MHD-free plasma and brain concentrations for a typical control, as compared with a seizing and verapamil-treated animal. Plasma MHD concentrations increased rapidly after bolus i.p. MHD administration, suggesting ready absorption from the peritoneal cavity. Maximal plasma concentrations were attained within 20 min. BBB penetration was rapid as MHD was already

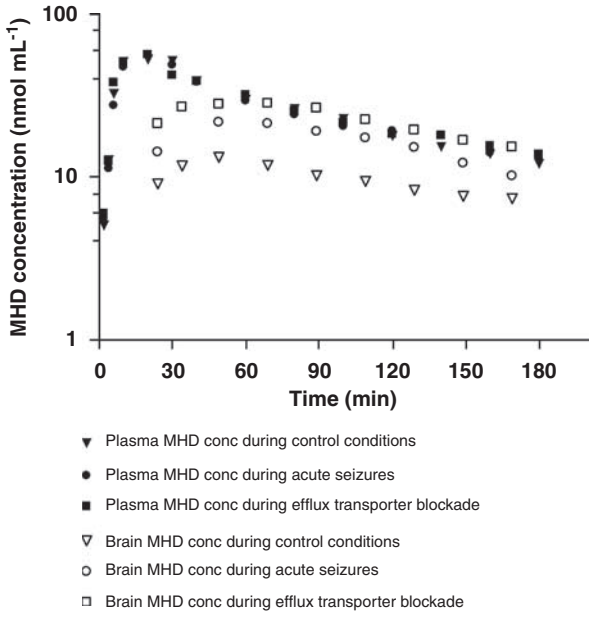


**Figure 2** Semilogarithmic plots of unbound plasma and brain extracellular (EC) fluid 10,11-dihydro-10-hydroxy-carbamazepine (MHD) concentration–time profiles following i.p. administration in a typical control rat, rat with pilocarpine-induced seizures and rat with concomitant efflux transport inhibition through intracerebral verapamil perfusion.

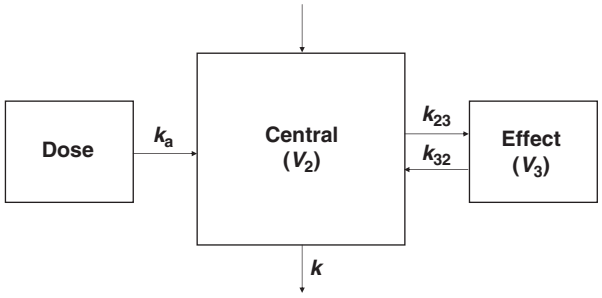


**Figure 3** A schematic overview of the population pharmacokinetic model for 10,11-dihydro-10-hydroxy-carbamazepine (MHD) describing the pharmacokinetics in plasma and brain simultaneously. The model consists of a central compartment with combined zero- and first-order absorption with lag time and biophase distribution ($V$, volume of distribution; $k_a$, absorption rate constant; $k$, elimination rate constant; $k_{23}$, $k_{32}$, transfer rate constants between central and effect compartment).

detectable at the time of first sampling (2 min post-dose). The maximal MHD levels in the hippocampus were observed within 60 min after drug administration. Plasma and brain concentrations increased linearly and dose-dependently, with subsequent first-order elimination. Biophase PK differed importantly from plasma PK, as BBB transport and brain distribution did not occur instantaneously (in all conditions) and to a full extent (in control conditions).

On the basis of model selection criteria, a one-compartment model with absorption and biophase distribution best described the concentration–time profile of MHD simultaneously in plasma and hippocampal ECF (Figure 3). The absorption after i.p. administration was characterized by a first-order process with lag time ($ALAG_1$). The nonlinearity in the absorption phase was described under the assumption of a hypothetical zero-order infusion (with duration $D_2$) for a fraction ($F_1$) of dose. This nonlinearity may be explained by the fact that MHD was administered as a suspension, which creates a depot from which a part of the compound is not instantly available for absorption. The difference in the brain volume of distribution ($V_3$) between control rats ($V_{3a}$), seizing rats ($V_{3b}$) and rats with efflux transport inhibition ($V_{3c}$) was statistically significant (Table 2). No significant effect of treatment was observed on the remaining model parameters. This finding indicates that the PK of MHD in the brain, but not in plasma, is significantly affected by acute seizures and efflux transport inhibition.

The final model enabled prediction of MHD plasma and brain concentrations for all study groups. The goodness-of-fit plots for the model are depicted in Figure 4. Individually observed MHD plasma and brain concentrations do not deviate substantially from individual and population model predictions. The conditional weighed residuals are randomly distributed around zero in concentration, indicating absence of bias.

All structural PK parameters were estimated precisely with acceptable coefficient of variation (<15%), with exception of WT (59.6%). Inter-subject variability could be characterized for $k_{23}$, $k_{32}$, $V_{3a}$, $V_{3c}$, $F_1$ and $D_2$. An overview of all model parameters and their respective coefficients of variation, inter-subject ($\omega^2$) and residual variability is provided in Table 2. During seizures, $V_{3b}$ decreased by about 30%, whereas $V_{3c}$ decreased by about 50% during efflux transport blockade, as compared with control conditions ($V_{3a}$).

**Table 2** Population mean pharmacokinetic parameter estimates of MHD in plasma and brain

| *Parameters* | *Original data set* | | *1395 bootstrap replicates* | |
|---|---|---|---|---|
| | *Estimate* | *CV%* | *Estimate* | *CV%* |
| *Structural model* | | | | |
| $k_a$ ($min^{-1}$) | 0.22 | 11.4 | 3.31 | 161.3 |
| $k$ ($min^{-1}$) | 0.0114 | 3.9 | 0.0115 | 2.7 |
| $k_{23}$ ($min^{-1}$) | 0.0203 | 14.4 | 0.0208 | 6.0 |
| $k_{32}$ ($min^{-1}$) | 0.0306 | 6.8 | 0.0306 | 2.8 |
| $V_2$ (mL) | 484 | 3.8 | 480.22 | 8.2 |
| $V_3$ (mL) | | | | |
| $V_{3a}$ (control) | **813** | 9.8 | **823.11** | 8.8 |
| $V_{3b}$ (acute seizures) | **563*** | 12.6 | **573.41*** | 11.9 |
| $V_{3c}$ (efflux inhibition) | **407*** | 13.4 | **416.43*** | 4.8 |
| $ALAG_1$ (min) | 3.23 | 4.6 | 3.23 | 18.0 |
| $F_1$ | 0.347 | 14.4 | 0.359 | 7.6 |
| $D_2$ (min) | 12.6 | 4.8 | 12.5 | 7.574 |
| WT | 0.0782 | 59.6 | 0.1433 | 122.3 |
| *Inter-animal variability* | | | | |
| $\omega^2$ $k_{23}$ | 0.14 | 32.9 | 0.132 | 26.8 |
| $\omega^2$ $k_{32}$ | 0.153 | 21.0 | 0.0914 | 60.4 |
| $\omega^2$ $V_{3a}$ | 0.078 | 28.3 | 0.15 | 19.0 |
| $\omega^2$ $V_{3c}$ | 0.0187 | 86.6 | 0.074 | 25.5 |
| $\omega^2$ $F_1$ | 0.0975 | 73.2 | 0.0811 | 66.6 |
| $\omega^2$ $D_2$ | 0.0575 | 33.9 | 0.063 | 27.2 |
| *Residual variability* | | | | |
| Proportional error plasma | 0.0256 | 17.6 | 0.0251 | 16.2 |
| Additive error plasma | 13.00 | 58.7 | 14.05 | 50.3 |
| Proportional error brain | 0.605 | 101.3 | 0.576 | 65.7 |

Abbreviations: $ALAG_1$, lag time; $D_2$, infusion duration; $F_1$, fraction of dose; MHD, 10,11-dihydro-10-hydroxy-carbamazepine; $k$, elimination rate constant; $k_{23}$, $k_{32}$, inter-compartmental transfer rate constants between plasma and brain; $k_a$, absorption rate constant; $V$, volume of distribution; WT, weighing factor.
*$P<0.05$.
One of our major modelling findings is that a change in convulsive state of the animals or efflux transport availability only translates into a significant change in brain volume of distribution. The values for these parameters are in bold to draw attention to this crucial result.

Bootstrapping and VPC were conducted as part of the model validation procedures. The final population PK estimates for MHD in plasma and brain were nearly identical to the estimates obtained by fitting 1395 (that is, number of successful runs out of 1500 analysis) data sets to the final population PK model (Table 2). The results of the VPC showed consistency in the estimation of plasma MHD levels, as indicated by an accurate prediction of >95% of the measured MHD plasma concentrations over time. The observed time course of MHD concentrations in the brain was also accurately predicted. However, the inter-subject variability in parameter estimates is somewhat overestimated as evidenced by the width of the quantiles. In Figure 5, the VPC plots are depicted for the 20 mg $kg^{-1}$ MHD group during control conditions, acute seizures and efflux transport inhibition. Figures 6 and 7 show the VPC results

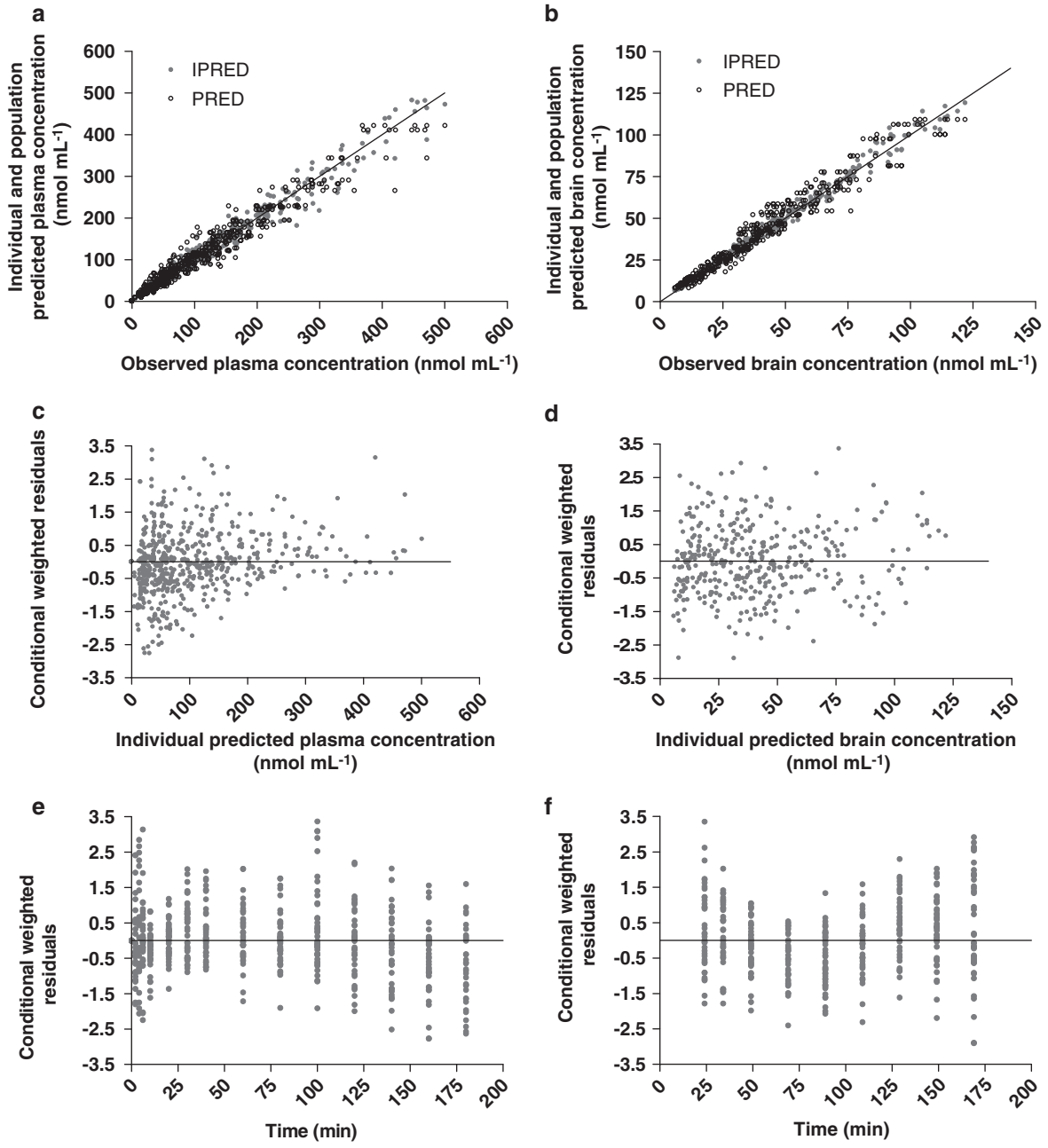


**Figure 4** Goodness-of-fit plots obtained for the final population pharmacokinetic model. Scatter plots show the observed 10,11-dihydro-10-hydroxy-carbamazepine (MHD) plasma (**a**) and brain (**b**) concentrations versus the individual (IPRED) and population (PRED) predictions; conditional weighed residuals (CWRES) are depicted against individual predicted plasma (**c**) and brain (**d**) concentration and against time for plasma (**e**) and brain (**f**).

obtained for subtherapeutic and anticonvulsant MHD doses, respectively.

## Discussion

This study was designed to characterize the disposition of the antiepileptic compound MHD in rat plasma and brain simultaneously using population PK modelling. In addition, we also explored in a strictly quantitative manner the influence of acute seizures and efflux transport mechanisms on distribution of MHD to the brain. A one-compartment PK model with combined zero- and first-order absorption, including lag time and biophase distribution was found to best describe simultaneously the disposition of MHD in plasma and brain over a wide dosing range (20–150 mg $kg^{-1}$). We show that the effect of acute seizures and efflux transport inhibition on MHD brain exposure can be parameterized in terms of changes in $V_3$. As $V_3$ is a parameter reflecting drug distribution in the biophase, we infer that changes in this

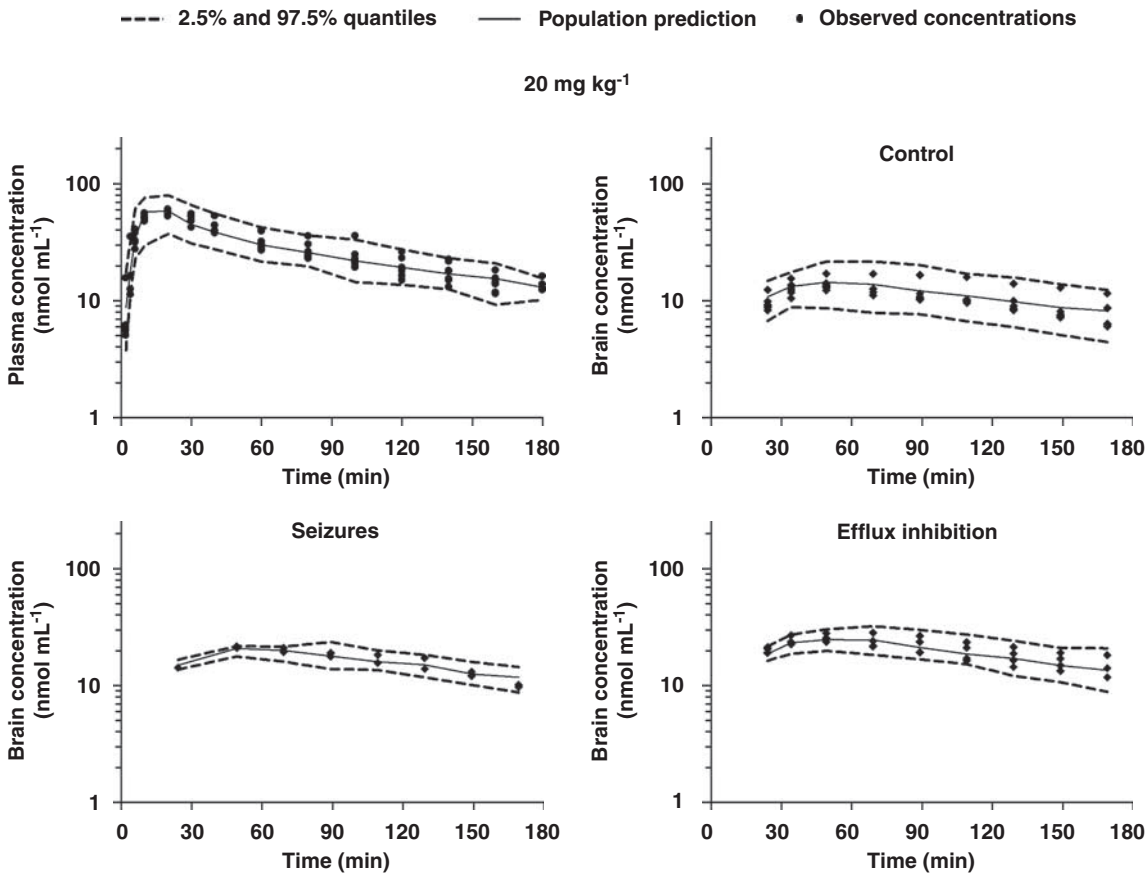


**Figure 5** Pharmacokinetics of 10,11-dihydro-10-hydroxy-carbamazepine (MHD) in plasma and brain in control conditions, during acute seizures and during efflux transport inhibition following i.p. administration of a subtherapeutic MHD dose (20 mg kg$^{-1}$). Observed values and population predictions with 2.5 and 97.5% quantiles are shown.

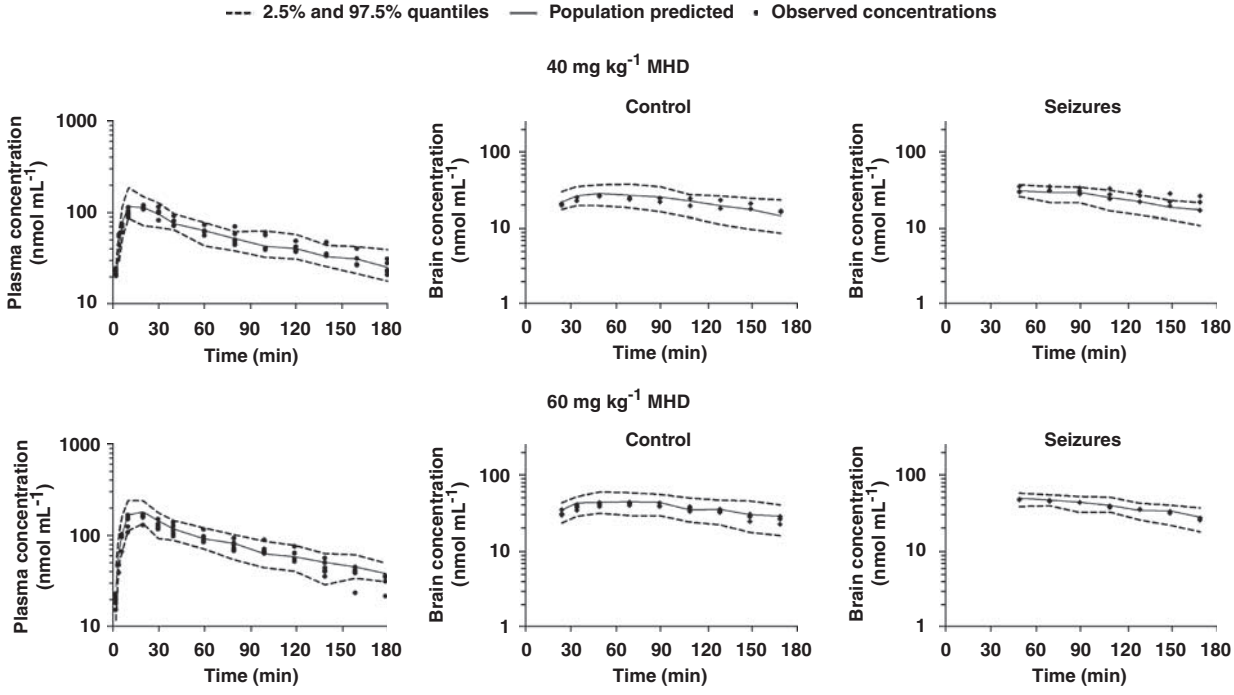


**Figure 6** Pharmacokinetics of 10,11-dihydro-10-hydroxy-carbamazepine (MHD) in plasma and brain in control conditions and during acute seizures following intraperitoneal administration of subtherapeutic MHD doses (40 and 60 mg kg$^{-1}$). Observed values and population predictions with 2.5 and 97.5% quantiles are shown for each dosing group.

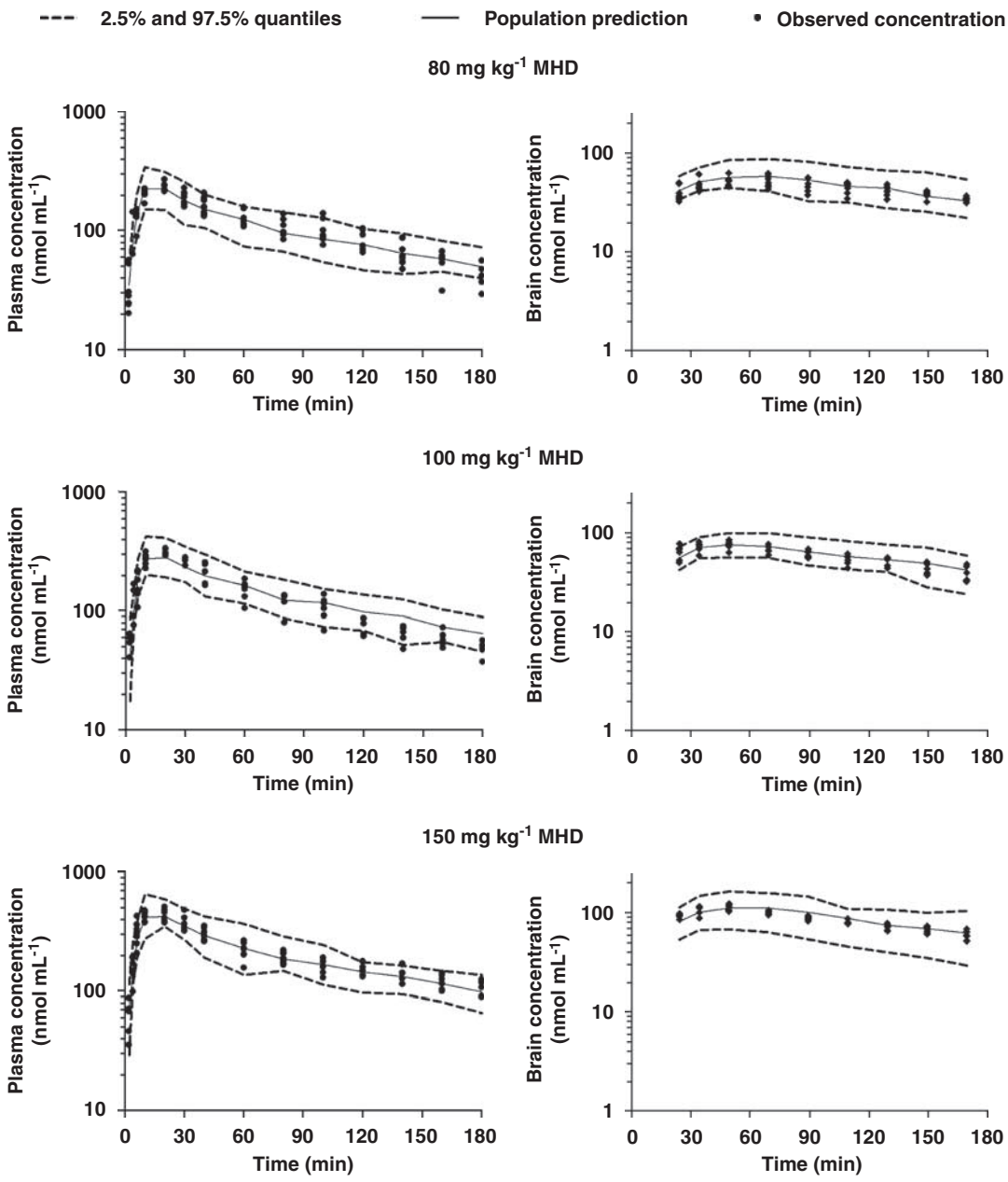


**Figure 7** Pharmacokinetics of 10,11-dihydro-10-hydroxy-carbamazepine (MHD) in plasma and brain in control conditions and during acute seizures following intraperitoneal administration of anticonvulsant MHD doses (80, 100 and 150 mg kg$^{-1}$). Observed values and population predictions with 2.5 and 97.5% quantiles are shown for each dosing group.

parameter can be used to quantify the impact of pathological processes on drug transfer across the BBB.

*Effect of acute seizures*

The significant increase in brain MHD concentrations during acute seizure activity might be related to altered passive brain entry due to a leaky BBB (Oby and Janigro, 2006). Also, increased local cerebral blood flow, which has been described in epileptic brain areas during seizures, can lead to increased MHD influx. In principle, an increase in BBB permeability should have been reflected in an increased $k_{23}$ value instead of a reduction in $V_3$, as observed from the covariate analysis. Possibly, the transient occurrence of seizure activity, which is inherent to the focal pilocarpine model, in combination with the somewhat long microdialysis sampling intervals (10–20 min) hampers the identification of rate constants, which are of a higher order of magnitude. As seizure activity was induced only transiently and subsides towards the end of the experiment, it is conceivable that only a part of the collected microdialysate samples reflects the changes in EC levels of MHD resulting from compromised BBB integrity and increased local cerebral blood flow. Alternatively, one should also consider that acute seizures may have affected both brain influx as well as efflux, such that there is minimal net perturbation of the bidirectional flux. Indeed, improved

passive entry may be tempered by compensatory mechanisms that are triggered by BBB disruption, such as vasogenic oedema in brain tissue and MDT overexpression (Oby and Janigro, 2006; van Vliet *et al*., 2007). On the other hand, the decrease in apparent brain volume of distribution could also suggest that seizure-induced redistribution phenomena within the brain are driving the increase in the EC drug concentration rather than improved brain influx.

*Effect of efflux transport inhibition*

In control conditions, MHD biophase distribution was limited, confirming the hypothesis that efflux transport of MHD is physiologically active at the BBB. The proposed modelling approach provided evidence that local administration of an efflux transport inhibitor increases the EC hippocampal concentrations of MHD. These data are in line with previous studies demonstrating increased brain ECF levels of AEDs following efflux transporter blockade *in vivo* (Clinckers *et al*., 2005; Löscher and Potschka, 2005; van Vliet *et al*., 2006, 2007). We have also shown that MDT inhibition is necessary to obtain anticonvulsant levels of oxcarbazepine in rat hippocampus (Clinckers *et al*., 2005). To date, two clinical studies have demonstrated that verapamil co-administration may improve the response to AED treatment in intractable patients (Summers *et al*., 2004; Iannetti *et al*., 2005). In addition, Marchi *et al*. (2005) suggested that in epileptic patients not responding to oxcarbazepine, P-glycoprotein-mediated efflux was responsible for the attainment of insufficient MHD concentrations at the neuronal targets, despite appropriate systemic exposure. Inhibition of active extrusion at the BBB is considered responsible for the increased ECF drug concentrations and hence improved PD response. In this respect, a decrease in $k_{32}$ parameter value relative to control group animals should have been identified by stepwise covariate inclusion during model building. Instead, a significant decrease in $V_3$ was identified, suggesting that the increase in the concentrations of MHD in ECF following intrahippocampal co-administration of verapamil may be caused by MHD redistribution processes within the brain. The cellular membranes of brain parenchymal cells, such as microglia and astrocytes, express influx and efflux transporters and are proposed to act as barriers for drug distribution (Lee *et al*., 2001).

We hypothesize that inhibition of parenchymal cell transporter systems by verapamil may be responsible for the presented increases in ECF levels of MHD. The lack of effect on the rate constant value, and hence on drug clearance from the biophase, may also imply that verapamil-insensitive MDTs are involved in the active efflux of MHD at the BBB or that verapamil may have equally inhibited influx and efflux mechanisms at the BBB. Further research is needed to unravel the impact of selective blockade of other MDT systems on the distributional characteristics of MHD.

*Simultaneous PK modelling: advantages and limitations*

Our results clearly show that combination of experimental techniques, such as microdialysis and PK sampling, with nonlinear mixed effects modelling yields valuable information about the brain disposition of CNS compounds, which cannot be obtained otherwise. In addition, the use of nonlinear mixed effects (also known as population modelling) enables simultaneous analysis of microdialysis and plasma data in all experimental groups. This approach has been pivotal to reach the conclusions of this study. In contrast to conventional non-compartmental analysis, nonlinear mixed effects modelling allows the estimation of population parameters (fixed effects), together with the corresponding variability (random effects), separating true inter-subject differences from residual noise. The main limitation in the current analysis is that inter-subject variability for the PK parameters describing biophase disposition has been poorly estimated, which is partly explained by the experimental setting. However, it is important to emphasize that estimates would not have been without artefact if brain data were analysed separately from plasma data.

To the best of our knowledge, this is the first time modelling has been used to describe both plasma and brain disposition of an antiepileptic compound. To date, published studies with AEDs have applied PK/PD modelling to *in vivo* data based on plasma PK only (Van der Graaf and Danhof, 1997; Cleton *et al*., 1999; Garrido *et al*., 2000) or performed separate analysis of the plasma and brain data (Groenendaal *et al*., 2007; Geldof *et al*., 2008). Because of simultaneous modelling of PK in plasma and in the brain, MHD disposition during seizures and efflux transport-mediated inhibition could be clarified unambiguously. This approach also accounts for the effect of potential differences in plasma PK on brain disposition. As BBB permeability disturbances following seizures are a dynamic phenomenon, we anticipate that this approach will provide evidence of time-dependent changes in brain disposition and redistribution of MHD and other compounds in chronic epileptic conditions in the post-status epilepticus model for mesial temporal lobe epilepsy. Furthermore, it is our intention to use this model to evaluate the effect of acute seizures and efflux transport inhibition on the PD and anticonvulsant effect of MHD.

*Implications for therapeutic drug monitoring*

As shown in Figure 2, ECF levels of MHD reach approximately the same level of free drug in plasma during acute seizures and efflux transport inhibition. The changes in biophase kinetics are reflected by the decrease in $V_{3b}$ and $V_{3c}$ without any implication to the parameter estimates associated with systemic drug disposition. Multidrug transporter overexpression has been described in epileptogenic brain tissue samples from pharmacoresistant patients and epileptic animals. This overexpression seems to occur preferentially in regions that are involved in seizure generation and spread, such as the ventral hippocampus (Kwan and Brodie, 2005; van Vliet *et al*., 2007). It is therefore assumed that AEDs are not equally distributed over the epileptic brain and that the access of AEDs to crucial regions is limited, leading to therapeutic failure despite adequate therapeutic plasma levels (Collins and Dedrick, 1983; Welty *et al*., 1993; Wang

and Welty, 1996; Hammarlund-Udenaes *et al*., 1997). Furthermore, it is also evident that the relation between plasma concentration and PD response can be highly variable from one patient to another and is highly affected by the type and severity of epilepsy (Schmidt and Haenel, 1984; Perucca, 2000).

The use of therapeutic drug monitoring is based on the assumption that systemic PK reflects target exposure and hence can be considered a surrogate for treatment response. The differences observed in brain kinetics during acute seizures and inhibition of efflux transport raise questions about the relevance of therapeutic drug monitoring in the pharmacological management of epilepsy. On the basis of the aforementioned findings, assessment of systemic exposure will not be predictive of patient response.

## Conclusion

To conclude, biophase disposition of AEDs may differ significantly from PK in plasma. BBB transport and brain distribution are restricted by the efflux transporters and altered by seizure activity. Our results show that the plasma–brain inter-relationship is altered during pathological conditions and that drug redistribution within the brain is likely to be involved. It is clear that characterization of target tissue distribution in control and pathological conditions is imperative for accurate dosing rationale. These factors can be easily taken into account in PK/PD modelling (Hammarlund-Udenaes *et al*., 1997; de Lange and Danhof, 2002). Simultaneous modelling of PK in plasma and biophase is therefore recommended to evaluate alterations in biophase disposition under pathological conditions.

## Acknowledgements

We acknowledge the excellent assistance of G Santen, R Berckmans, G De Smet, C De Rijck and RM Geens. We thank the Fund for Scientific Research Flanders (FWO-Vlaanderen-Belgium) and the Vrije Universiteit Brussel for financial support. R Clinckers is a postdoctoral fellow of the FWO-Vlaanderen.

## Conflict of interest

The authors state no conflict of interest.

## References

Beal SL, Sheiner LB (1999). *NONMEM Users Guide*. University of California: San Francisco, CA.

Bebawy M, Morris M, Roufogalis B (2001). Selective modulation of P-glycoprotein-mediated drug resistance. *Br J Cancer* **85**: 1998–2003.

Benveniste H, Hüttemeier P (1990). Microdialysis—theory and application. *Prog Neurobiol* **35**: 195–215.

Clapp-Lilly K, Roberts R, Duffy L, Irons K, Hu Y, Drew K (1999). An ultrastructural analysis of tissue surrounding a microdialysis probe. *J Neurosci Methods* **90**: 129–142.

Cleton A, de Greef H, Edelbroek P, Voskuyl R, Danhof M (1999). Application of a combined 'effect compartment/indirect response model' to the central nervous system effects of tiagabine in the rat. *J Pharmacokinet Biopharm* **27**: 301–323.

Clinckers R, Smolders I, Meurs A, Ebinger G, Michotte Y (2005). Quantitative *in vivo* microdialysis study on the influence of multidrug transporters on the blood–brain barrier passage of oxcarbazepine: concomitant use of hippocampal monoamines as pharmacodynamic markers for the anticonvulsant activity. *J Pharmacol Exp Ther* **314**: 725–731.

Collins J, Dedrick R (1983). Distributed model for drug delivery to CSF and brain tissue. *Am J Physiol* **245**: R303–R310.

Danhof M, de Lange EC, Della Pasqua OE, Ploeger BA, Voskuyl RA (2008). Mechanism-based pharmacokinetic–pharmacodynamic (PK–PD) modeling in translational drug research. *Trends Pharmacol Sci* **29**: 186–191.

de Lange E, Danhof M (2002). Considerations in the use of cerebrospinal fluid pharmacokinetics to predict brain target concentrations in the clinical setting: implications of the barriers between blood and brain. *Clin Pharmacokinet* **41**: 691–703.

Ette E, Williams P, Kim Y, Lane J, Liu M, Capparelli E (2003). Model appropriateness and population pharmacokinetic modeling. *J Clin Pharmacol* **43**: 610–623.

Garrido M, Gubbens-Stibbe J, Tukker E, Cox E, von Frijtag J, Künzel D *et al*. (2000). Pharmacokinetic–pharmacodynamic analysis of the EEG effect of alfentanil in rats following beta-funaltrexamine-induced mu-opioid receptor 'knockdown' *in vivo*. *Pharm Res* **17**: 653–659.

Geldof M, Freijer J, van Beijsterveldt L, Danhof M (2008). Pharmacokinetic modeling of non-linear brain distribution of fluvoxamine in the rat. *Pharm Res* **25**: 792–804.

Groenendaal D, Freijer J, de Mik D, Bouw M, Danhof M, de Lange E (2007). Population pharmacokinetic modelling of non-linear brain distribution of morphine: influence of active saturable influx and P-glycoprotein mediated efflux. *Br J Pharmacol* **151**: 701–712.

Hammarlund-Udenaes M, Paalzow L, de Lange E (1997). Drug equilibration across the blood–brain barrier—pharmacokinetic considerations based on the microdialysis method. *Pharm Res* **14**: 128–134.

Hooker A, Staatz C, Karlsson M (2007). Conditional weighted residuals (CWRES): a model diagnostic for the FOCE method. *Pharm Res* **24**: 2187–2197.

Iannetti P, Spalice A, Parisi P (2005). Calcium-channel blocker verapamil administration in prolonged and refractory status epilepticus. *Epilepsia* **46**: 967–969.

Iwi G, Millard R, Palmer A, Preece A, Saunders M (1999). Bootstrap resampling: a powerful method of assessing confidence intervals for doses from experimental data. *Phys Med Biol* **44**: N55–N62.

Kwan P, Brodie M (2005). Potential role of drug transporters in the pathogenesis of medically intractable epilepsy. *Epilepsia* **46**: 224–235.

Larsson C (1991). The use of an 'internal standard' for control of the recovery in microdialysis. *Life Sci* **49**: PL73–PL78.

Lee G, Dallas S, Hong M, Bendayan R (2001). Drug transporters in the central nervous system: brain barriers and brain parenchyma considerations. *Pharmacol Rev* **53**: 569–596.

Löscher W (2002). Current status and future directions in the pharmacotherapy of epilepsy. *Trends Pharmacol Sci* **23**: 113–118.

Löscher W, Potschka H (2005). Drug resistance in brain diseases and the role of drug efflux transporters. *Nat Rev Neurosci* **6**: 591–602.

Marchi N, Guiso G, Rizzi M, Pirker S, Novak K, Czech T *et al*. (2005). A pilot study on brain-to-plasma partition of 10,11-dihydro-10-hydroxy-5*H*-dibenzo(*b*,*f*)azepine-5-carboxamide and MDR1 brain expression in epilepsy patients not responding to oxcarbazepine. *Epilepsia* **46**: 1613–1619.

Oby E, Janigro D (2006). The blood–brain barrier and epilepsy. *Epilepsia* **47**: 1761–1774.

Paxinos G, Watson C (1986). *The Rat Brain in Stereotaxic Coordinates*, 2nd edn. Academic Press: San Diego, CA.

Perucca E (2000). Is there a role for therapeutic drug monitoring of new anticonvulsants? *Clin Pharmacokinet* **38**: 191–204.

Scheller D, Kolb J (1991). The internal reference technique in microdialysis: a practical approach to monitoring dialysis efficiency and to calculating tissue concentration from dialysate samples. *J Neurosci Methods* **40**: 31–38.

Schmidt D, Haenel F (1984). Therapeutic plasma levels of phenytoin, phenobarbital, and carbamazepine: individual variation in relation to seizure frequency and type. *Neurology* **34**: 1252–1255.

Scism J, Powers K, Artru A, Lewis L, Shen D (2000). Probenecid-inhibitable efflux transport of valproic acid in the brain parenchymal cells of rabbits: a microdialysis study. *Brain Res* **884**: 77–86.

Sheiner L, Grasela T (1991). An introduction to mixed effect modelling—concepts, definitions, and justification. *J Pharmacokinet Biopharm* **19**: S11–S24.

Summers M, Moore J, McAuley J (2004). Use of verapamil as a potential P-glycoprotein inhibitor in a patient with refractory epilepsy. *Ann Pharmacother* **38**: 1631–1634.

Van Belle K, Verfaillie I, Ebinger G, Michotte Y (1995). Liquid chromatographic assay using a microcolumn coupled to a U-shaped optical cell for high-sensitivity ultraviolet absorbance detection of oxcarbazepine and its major metabolite in microdialysates. *J Chromatogr B Biomed Appl* **672**: 97–102.

Van der Graaf P, Danhof M (1997). Analysis of drug–receptor interactions *in vivo*: a new approach in pharmacokinetic–pharmacodynamic modelling. *Int J Clin Pharmacol Ther* **35**: 442–446.

van Vliet E, van Schaik R, Edelbroek P, Redeker S, Aronica E, Wadman W *et al*. (2006). Inhibition of the multidrug transporter P-glycoprotein improves seizure control in phenytoin-treated chronic epileptic rats. *Epilepsia* **47**: 672–680.

van Vliet E, van Schaik R, Edelbroek P, Voskuyl R, Redeker S, Aronica E *et al*. (2007). Region-specific overexpression of P-glycoprotein at the blood–brain barrier affects brain uptake of phenytoin in epileptic rats. *J Pharmacol Exp Ther* **322**: 141–147.

Wählby U, Jonsson E, Karlsson M (2001). Assessment of actual significance levels for covariate effects in NONMEM. *J Pharmacokinet Pharmacodyn* **28**: 231–252.

Wang Y, Welty D (1996). The simultaneous estimation of the influx and efflux blood–brain barrier permeabilities of gabapentin using a microdialysis–pharmacokinetic approach. *Pharm Res* **13**: 398–403.

Welty D, Schielke G, Vartanian M, Taylor C (1993). Gabapentin anticonvulsant action in rats: disequilibrium with peak drug concentrations in plasma and brain microdialysate. *Epilepsy Res* **16**: 175–181.

Yano Y, Beal S, Sheiner L (2001). Evaluating pharmacokinetic/pharmacodynamic models using the posterior predictive check. *J Pharmacokinet Pharmacodyn* **28**: 171–192.